PERGAMON

International Journal of Solids and Structures 38 (2001) 2033–2047

INTERNATIONAL JOURNAL OF SOLIDS and STRUCTURES

www.elsevier.com/locate/ijsolstr

Finite axisymmetric deformations of an initially stressed fluid-filled cylindrical membrane

D. Pamplona [a,*], P. Gonçalves [a,1], M. Davidovich [a], H.I. Weber [b]

[a] *Civil Engineering Department, Catholic University, PUC-Rio 33452-900, Rio de Janeiro, Brazil*
[b] *Mechanical Engineering Department, Catholic University, PUC-Rio 22453-900, Rio de Janeiro, Brazil*

Received 6 October 1999; in revised form 2 February 2000

Abstract

This paper investigates the large deformations of an extended fluid-filled cylindrical membrane. The static case and the behaviour of the membrane rotating at a constant angular velocity are both considered. A detailed experimental analysis was carried out involving different geometries, and initial axial forces and the influence of the axial force and the fluid volume were investigated. An apparatus was developed to support vertically the extended cylindrical membrane while it is filled with liquid. The membrane used in these experiments is composed of an isotropic, homogeneous and elastic rubber, which is modelled as a neo-Hookean incompressible material, described by a single elastic constant. This constant was obtained by comparing the experimental and numerical solutions for the membrane under traction. The differential equilibrium equations for this specific problem and material were derived and solved by the shooting method. When the extended membrane was filled with liquid, it was observed that the height of liquid increased initially as the volume of liquid inside the membrane increased until a certain critical height was reached after which it remained constant or decreased slightly with increasing volume, up to the moment when the membrane lost its stability into a non-symmetric mode. These experimental results are, as shown in the paper, in satisfactory agreement with the theory.

Keywords: Cylindrical membrane; Finite deformations; Fluid-filled membrane; Neo-Hookean material

1. Introduction

The pioneering work of Green and Adkins (1960) on non-linear elasticity set up the basis for the analysis of membranes under large deformations. Since then many important papers have been published in this field, most of which deal with the equilibrium and stability of cylindrical and spherical membranes under uniform pressure loading or loads acting along the boundaries (Corneliussen and Shield, 1961; Alexander,

* Corresponding author. Tel.: +55-21-529-9346; fax: +55-21-511-1546.
E-mail addresses: djenane@civ.puc-rio.br (D. Pamplona), paulo@civ.puc-rio.br (P. Gonçalves).
[1] Also Corresponding author. Civil Engineering Department, Catholic University - PUC-Rio 22453-900 Rio de Janeiro, Brazil.

0020-7683/01/$ - see front matter
PII: S0020-7683(00)00151-7

1971; Haughton and Ogden, 1978; Ratner, 1983; Li and Steigmann, 1993; Haseganu and Steigmann, 1994; Chen, 1995). It should be pointed out that the number of experimental contributions to this class of problems is small compared with the theoretical and numerical ones. Among the experimental investigations in this field, the publications of Green and Adkins (1960), Alexander (1971) and Pamplona and Bevilacqua (1992) should be mentioned.

The analysis of large deformations of fluid-filled membranes is not so popular; nevertheless, there are some important publications such as the ones by Yu and Valanis (1970) and Boyer and Gutkowski (1970) and, more recently, the work of Haughton (1996). The linear, small deformation analysis, of fluid-filled membranes is more common in literature (Ohyama et al., 1989; Zhao, 1995). Nonetheless, fluid-filled membranes are found in several engineering fields. Of particular importance is the recent interest in the use of membranes as containers for the storage and transportation of fluids (Isaacson, 1987) and also as a barrier for wave attenuation in severe environment (Zhao, 1995; Williams, 1996). Also, the understanding of the static and dynamic behaviour of fluid-filled membranes is important in biology and bioengineering, since fluid-filled membranes of various geometries are found in all living organisms (Evans and Skalak, 1981; Secomb and Gross, 1983; Pamplona and Calladine, 1993). These structures are load adaptive, as they change their geometry to accommodate external loads with the minimum variation in stress levels, and therefore, may be an efficient engineering solution in many practical fields. In most of these applications, the non-linearities of deformation and material response are very important. In this work, we investigate the non-linear behaviour of extended fluid-filled cylindrical membranes suitably supported, both theoretically and experimentally. The static case and the behaviour of the membrane rotating at a constant angular velocity are both considered. In the theoretical formulation of the problem, the membrane is considered to be incompressible, homogeneous, isotropic and neo-Hookean when subjected to large deformations. This is in agreement with the physical characteristics of the rubber membranes used in the experimental investigation. In the experimental analysis, several geometries and loading cases were investigated, and these results were compared with the theoretical results obtained by solving the non-linear equilibrium equation by the so-called shooting method, using the Runge–Kutta and Newton–Raphson algorithms.

The experimental and theoretical results compare well with each other and show some interesting features. Different traction forces acting on cylindrical membranes with the same dimensions exhibit a critical volume, or liquid height, after which the height of the liquid maintains itself constant or decreases slightly with increasing volume. Increasing the amount of fluid still further, there is another critical volume at which the membrane loses its axisymmetrical shape.

2. Problem formulation

Throughout this paper, a homogeneous, isotropic, hyperelastic cylindrical membrane of initial radius A, length L_0^*, and constant initial thickness H^* is considered. Henceforth, a superposed star denotes a dimensional quantity. In the deformed configuration, both ends are fixed to two circular rigid rings also of radius A and separated by a distance l_0^*. The membrane is filled with an inviscid and incompressible fluid of specific weight γ^* to a height l_w^* The co-ordinates of a typical point P_o, on the middle surface of the undeformed membrane, are R^* and Z^*. Since the membrane is cylindrical, R^* is constant and equal to A. The co-ordinates of the same typical point, P, in the deformed configuration are denoted by r^* and z^*. Since only axisymmetric deformations are considered, all variables are independent of the circumferencial co-ordinate. The deformed and undeformed thickness of the membrane are h^* and H^*, respectively, and s^* is the arc length along a meridian of the deformed membrane. The co-ordinate Z^* is taken as the independent variable, in such a way that all deformed variables are a function of Z^*. The relevant geometrical parameters are shown in Fig. 1.

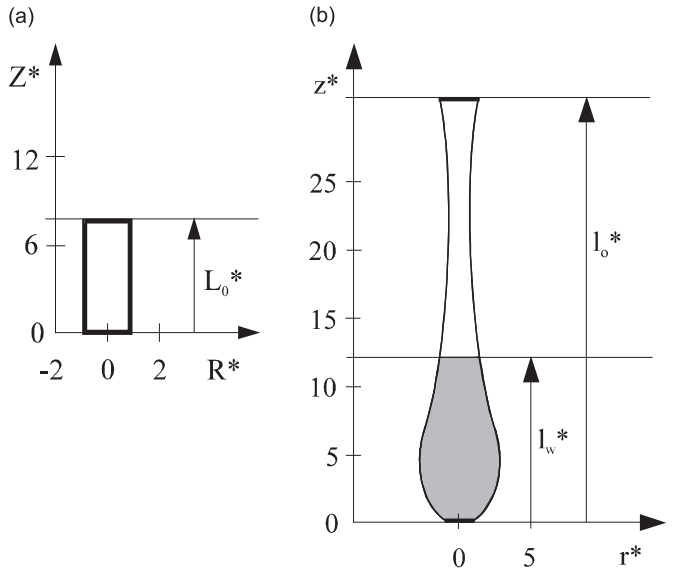

Fig. 1. Fluid-filled cylindrical membrane: (a) undeformed and (b) deformed configuration.

For axially symmetric problems, the extension ratios in the principal directions, λ_1, λ_2 and λ_3, are

$$\lambda_1 = \frac{r^*}{A}, \qquad \lambda_2 = \frac{\mathrm{d}s^*}{\mathrm{d}Z^*} = \sqrt{(r^*)'^2 + (z^*)'^2}, \qquad \lambda_3 = \frac{h^*}{H^*}, \tag{1}$$

where $(\ )'$ are derivatives with respect to Z^*.

2.1. Boundary conditions

The boundary conditions at the edges of the cylinder are

$$\text{at } Z^* = 0, \quad r^* = A \text{ and } z^* = 0, \tag{2}$$

$$\text{at } Z^* = L_0^*, \quad r^* = A \text{ and } z^* = l_0^*. \tag{3}$$

2.2. Equilibrium equations

The equilibrium equations for axially symmetric membranes along the tangent and normal directions are given, respectively, by (Green and Adkins, 1960)

$$\frac{\mathrm{d}}{\mathrm{d}s^*}(T_1^* r^*) = T_2^* \frac{\mathrm{d}r^*}{\mathrm{d}s^*}, \tag{4}$$

$$K_1^* T_1^* + K_2^* T_2^* = p^*. \tag{5}$$

Here, T_2^* and T_1^* are the meridional and circumferential stresses, respectively, and K_2^* and K_1^* are the associated radii of curvature; p^* is the hydrostatic pressure loading normal to the deformed middle surface of the membrane plus the action of the angular velocity. The pressure p^* is considered to be positive when acting in the outward direction and can be written as

$$p^* = \gamma^*(z^* - l_w^*) + \frac{\gamma^*}{2g}\omega^2 r^2 \quad \text{for } z^* \leqslant l_w^*, \tag{6}$$

$$p^* = 0 \quad \text{for } z^* > l_w^*.$$

Here, γ^* is the specific weight of the liquid, g, the gravitational acceleration, ω, the angular velocity and l_w^*, the height of the liquid.

The principal radii of curvature, K_1^* and K_2^*, can be obtained from the following relations:

$$K_1^* = -\frac{\frac{d^2 r^*}{ds^{*2}}}{\sqrt{1 - \left(\frac{dr^*}{ds^*}\right)^2}}, \tag{7}$$

$$r^* K_2^* = \sqrt{1 - \left(\frac{dr^*}{ds^*}\right)^2}, \tag{8}$$

where $ds^* = \lambda_2 dZ^*$.

The meridional and circumferential stresses can be written in terms of the principal stretches as

$$T_2^* = h^* \lambda_1 W_1^*, \tag{9}$$

$$T_1^* = h^* \lambda_2 W_2^*. \tag{10}$$

Here, W^* is the constitutive relation of the membrane's material and W_1^* and W_2^* are the derivatives of W^* with respect to λ_1 and λ_2.

It is now assumed that the cylindrical membrane is made of a neo-Hookean incompressible material, whose strain energy density function is given by

$$W^* = C_1(\lambda_1^2 + \lambda_2^2 + \lambda_3^2 - 3), \tag{11}$$

where C_1 is the material elastic constant (the classical shear modulus). This equation provides a simple but realistic model for a rubber-elastic type material. As shown by Treolar (1975), statistical mechanical calculations on the configurations of long molecular chains lead precisely to equations of the type (11).

Using these relations, the differential equations (4) and (5) can be rewritten as

$$\lambda_2' W_{22} + \lambda_1' \left[W_{21} - \frac{W_2}{\lambda_1} \right] + \frac{r'}{r\lambda_2}[\lambda_2 W_2 - \lambda_1 W_1] = 0, \tag{12}$$

$$\lambda_2 W_2 \frac{r''z' - r'z''}{\sqrt{(r'^2 + z'^2)^3}} - \frac{\lambda_1 W_1 z'}{r\sqrt{r'^2 + z'^2}} + p = 0. \tag{13}$$

The above variables without superscript (*) are in dimensionless form, obtained from the division of the associated dimensional quantities by the initial membrane's radius, A. The non-dimensional pressure, p, is given by

$$p = \frac{\gamma^* A^2}{2C_1 H^*}\left[(z - l_w) + \frac{A\omega^2 r^2}{2g}\right]. \tag{14}$$

The non-dimensional boundary conditions are:

$$z(0) = 0, \qquad r(0) = 1, \tag{15}$$

$$z(L_0) = l_0, \qquad r(L_0) = 1. \tag{16}$$

2.3. Numerical solution

The problem described by Eqs. (12) and (13) and boundary conditions (15) and (16) is a fourth-order non-linear two point boundary value problem with two specified boundary conditions at each boundary.

In order to obtain the numerical solution of the problem, system (12) and (13) is first transformed into the following set of first order differential equations:

$$z' = u, \tag{17}$$

$$r' = v, \tag{18}$$

$$z'' = u' = (Fr' + Gz')/(r'^2 + z'^2)^2, \tag{19}$$

$$r'' = v' = (Fz' - Gr')/(r'^2 + z'^2)^2, \tag{20}$$

where u and v are auxiliary variables and

$$F = \frac{\lambda_1}{W_{22}}\left\{\lambda_1'\left[\frac{W_2}{\lambda_1}\right] - \frac{r'}{r\lambda_2}[\lambda_2 W_2 - \lambda_1 W_1]\right\}, \tag{21}$$

$$G = \frac{\lambda_2^2}{W_2}\left[W_1\frac{z'}{\lambda_2} - pr\lambda_2\right]. \tag{22}$$

The numerical solution of this problem is performed here by the shooting method (Keller, 1968; Press et al. 1986), which has been successfully used for the numerical solution of non-linear boundary value problems (Krayterman, 1990; Pamplona and Bevilacqua, 1992; Dos Anjos and Gonçalves, 1996). This method reduces the solution of a boundary value problem to the iterative solution of an initial value problem.

To define the initial value problem, the following set of initial conditions are prescribed at $Z = 0$:

$$z(0) = 0, \quad r(0) = 1, \quad u(0) = \tilde{u}, \quad v(0) = \tilde{v}, \tag{23}$$

where $\tilde{u}$ and $\tilde{v}$ are the unknown.

This approach involves a trial-and-error procedure. At the starting point, values are assumed for $\tilde{u}$ and $\tilde{v}$, and then the ordinary differential equations are solved by the fourth-order Runge–Kutta integration scheme, arriving at the other boundary. Unless the computed solution agrees with the known boundary conditions at the other end of the membrane ($z(L_0) = l_0,\ r(L_0) = 1$), the initial unknown conditions $\tilde{u}$ and $\tilde{v}$ are adjusted using the Newton–Raphson method, and the process is repeated until the assumed initial conditions yield, within specified tolerances, a solution that agrees with the known boundary conditions at the end of the integration interval.

3. Experimental analysis

Two pairs of aluminium rings were fabricated to hold the two edges of the cylindrical membrane, as shown in Fig. 2a. These two rings are attached to the metal frame shown in Fig. 2b in such a way that the cylindrical membrane can be stretched in the axial direction, as seen in Fig. 3. The membrane is filled with water through the upper hollow ring. The two rings are connected by a shaft, which can be rotated as a rigid body.

The cylindrical membrane used in these experiments is an isotropic, homogeneous rubber membrane of undeformed radius $A = 1.62$ cm and thickness $H^* = 0.005$ cm. The elastic material constants were obtained comparing the experimental and numerical solutions for the membrane under traction. Considering the

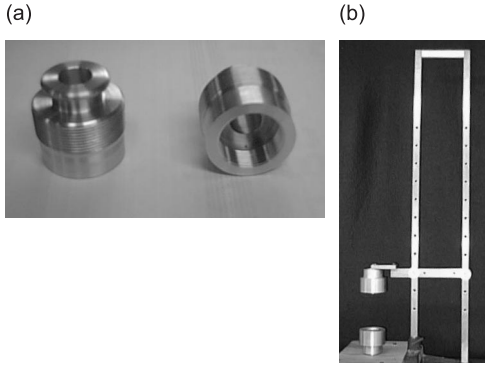

Fig. 2. Experimental apparatus.

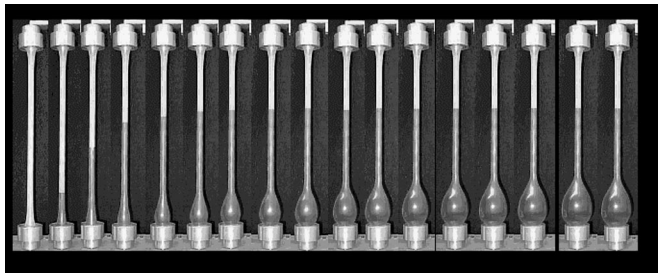

Fig. 3. Sequence of equilibrium configurations. $L_0^* = 11.6$ cm; $l_0^* = 51.6$ cm. Volume of water varying from 0 to 480 ml at every 30 ml.

material to be neo-Hookean, the material constant is found to be $C_1 = 2.424 \times 10^5$ Pa. The membrane is filled with water, so the specific weight $\gamma^* = 0.01$ N/cm^3.

A detailed parametric experimental analysis is conducted for different initial membrane lengths, L_0^*, initial tractions and liquid heights. Each experiment was repeated several times to check the results, and they proved to be perfectly reproducible.

3.1. Static analysis

First, for a given value of L_0^*, the membrane was stretched up to a desired length l_0^* and then filled slowly with water and the relation between the height of water, l_w^*, and the associated volume, V^*, was measured. The results for $L_0^* = 11.6$ cm and $L_0^* = 16.6$ cm are shown in Figs. 4 and 5, respectively. As one can observe from both figures, for each value of l_0^* ($l_0^* = 36.6$, 41.6, 46.6, and 51.6 cm), the height of the liquid increases as the volume increases and asymptotically tends to a maximum height. At these points, the addition of more water causes increased symmetric deformations but the liquid height and consequently the hydrostatic pressure remains practically constant up to a critical volume where the axisymmetric response becomes unstable and the membrane assumes an asymmetric equilibrium configuration. Comparing the results shown in Figs. 4 and 5, one can conclude that the relation between l_w^* and V^* as well as the maximum height are a function of the ratio of the stretched height of the tube to its original length, $\Delta_2 = l_0^*/L_0^*$. It should be pointed out that the overall extension ratio Δ_2 is not actually equal to the local value of extension ratio λ_2 because, as shown in Fig. 3, conditions along the tube are not uniform. For relatively low values of the extension ratio, the response is practically the same, but for large values of $\Delta_2 = l_0^*/L_0^*$, the maximum

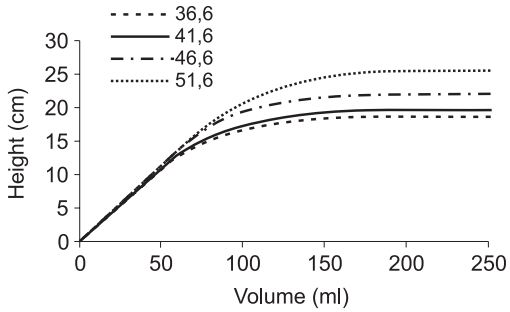

Fig. 4. Variation of the liquid height, l_w, as a function of the liquid volume, V^*. $L_0^* = 11.6$ cm (static loading: experimental results).

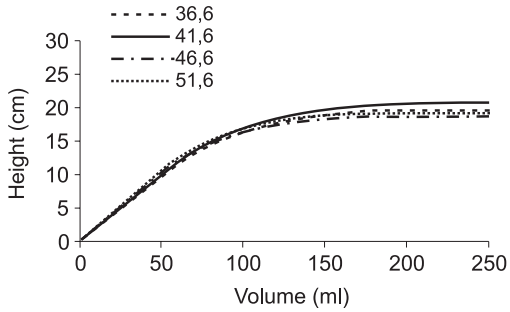

Fig. 5. Variation of the liquid height, l_w, as a function of the liquid volume, V^*. $L_0^* = 16.6$ cm (static loading: experimental results).

height increases as seen in Fig. 4 for $l_0^* = 46.6$ cm and $l_0^* = 51.6$ cm. During the experiments it was observed that this phenomenon could not be observed in membranes of initial length 5.6 cm or less, no matter what its final stretched length is. In these cases, the membranes is filled up with water before a maximum height (or pressure) is reached. This is just because the height of the apparatus (water column) is not large enough to generate sufficient pressure to push out a bulb at the bottom of the tube. It seems that the overall behaviour for a given initial stretch does not depend on the absolute height of the tube, provided that height is sufficient to generate enough water pressure.

A typical sequence of equilibrium configurations is illustrated in Fig. 3. These photographs are for $L_0^* = 11.6$ cm, $l_0^* = 51.6$ cm and for increasing volumes of water, ranging from 0 to 480 ml, at every 30 ml.

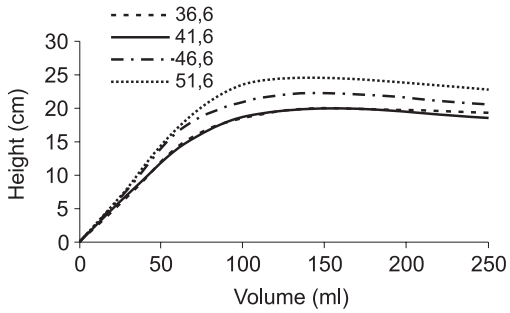

Fig. 6. Variation of the liquid height, l_w, as a function of the liquid volume, V^*. $L_0^* = 11.6$ cm. Membrane rotating at a constant angular velocity, $\omega = 40$ rad/s (experimental results).

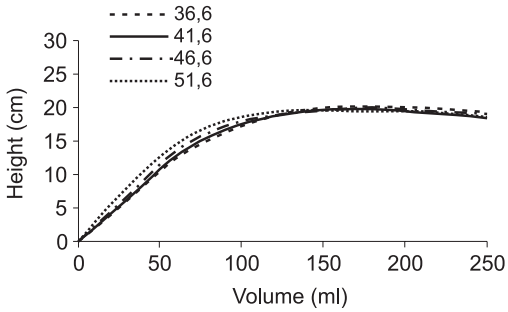

Fig. 7. Variation of the liquid height, l_w, as a function of the liquid volume, V^*. $L_0^* = 16.6$ cm. Membrane rotating at a constant angular velocity, $\omega = 40$ rad/s (experimental results).

3.2. Dynamic analysis

Now the behaviour of the liquid-filled membrane rotating at a constant angular velocity ω is analysed. The elastic liquid-filled membrane will present now an equilibrium configuration due to the combination of the gravitational field and the fluid centrifugal forces. The experiments were performed with a constant speed $\omega = 40$ rad/s, which is in a range where one expects that both effects have a similar magnitude. When the apparatus is rotating, the free surface of the fluid adopts a parabolic profile. This small difference is not considered in the calculations, since the free surface is always a rather narrow part of the tube. The results are presented in Figs. 6 and 7, using the same geometries analysed previously. In this case, the response is

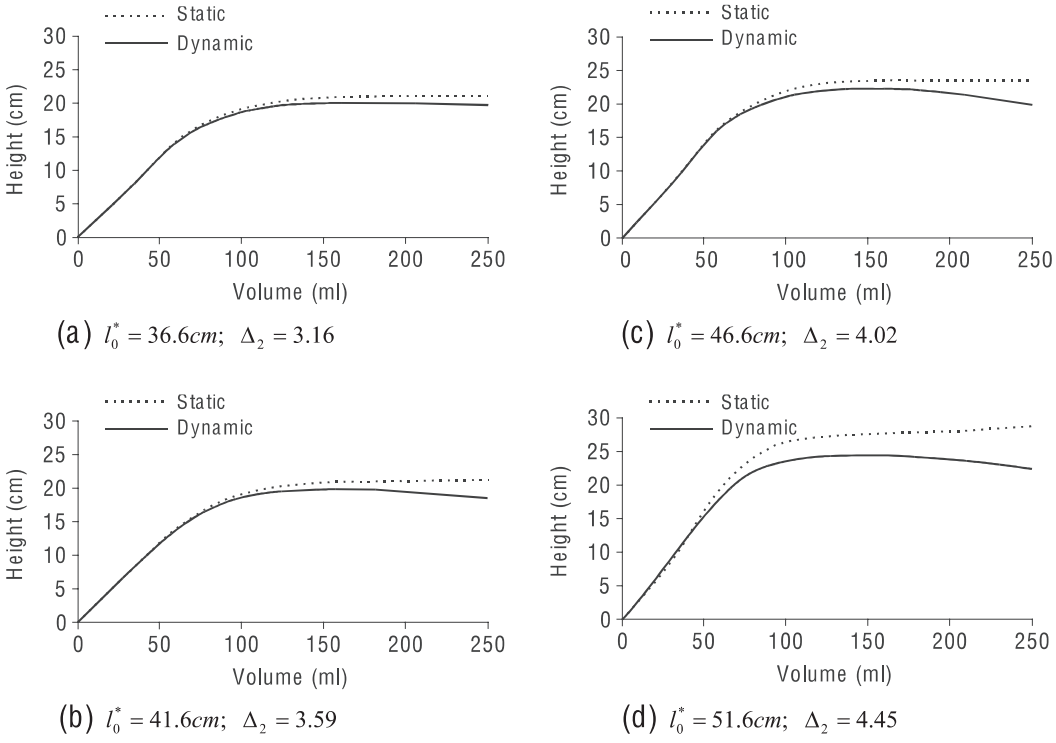

Fig. 8. Experimental analysis: comparision between static and dynamic results, $L_0^* = 11.6$ cm.

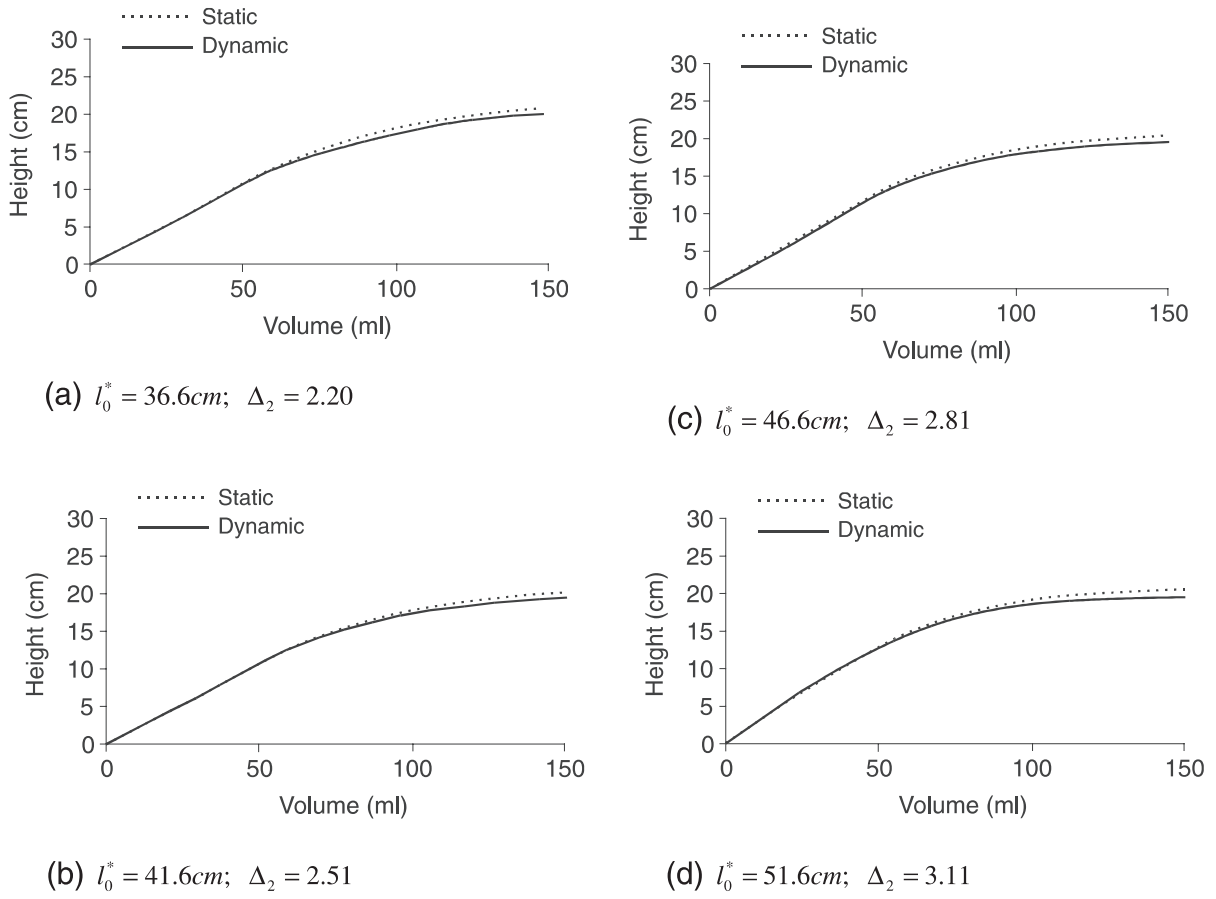

Fig. 9. Experimental analysis: comparison between static and dynamic results, $L_0^* = 16.6$ cm.

slightly different from the static case. First, the liquid height increases as the liquid volume increases but after reaching a maximum value, it decreases slowly as the volume increases. That is, after this limit point, the addition of more liquid results in a decrease in the hydrostatic pressure. Here again, a loss of stability of the symmetric configuration into a non-symmetric mode was observed. One can observe that the initial stretching has a similar influence on the response as for the static case.

A comparison between the static and dynamic response for each membrane geometry is shown in Figs. 8 and 9 for $L_0^* = 11.6$ cm and $L_0^* = 16.6$ cm, respectively. In all eight figures it is possible to observe that the relation between l_w^* and V^* is practically the same along the initial ascending branch, but the difference between the two curves increases as the liquid volume increases, showing the marked difference in behaviour for large values of V^*. This difference is more prominent for large values of Δ_2 as observed in Fig. 8c and d.

4. Numerical results

The same problem analysed experimentally were now solved using the formulation and numerical methodology presented in Section 2. The numerical results were obtained by assuming a height of water

and calculating, after convergence of the numerical process, the related volume. During the analysis, it was verified that it was more convenient to control numerically the height of water than its volume.

The results of the static analysis for $L_0^* = 11.6$ cm and $L_0^* = 16.6$ cm are shown in Figs. 10 and 11, respectively, where again the liquid height, l_w^*, is plotted as a function of the liquid volume, V^*, for different

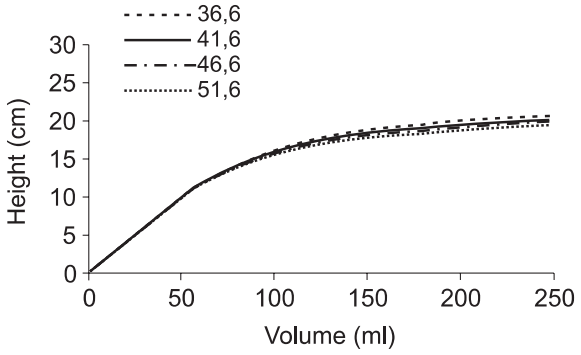

Fig. 10. Varaition of the liquid height, l_w, as a function of the liquid volume, V^* and $L_0^* = 11.6$ cm (static loading: numerical results).

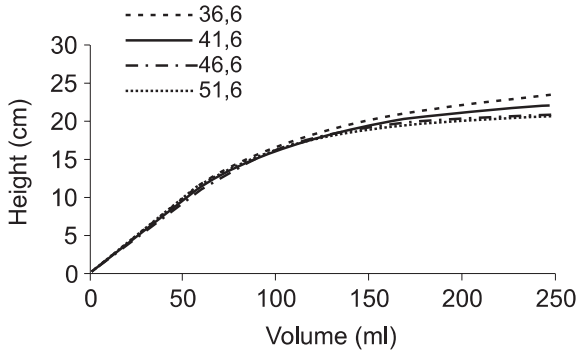

Fig. 11. Varaition of the liquid height, l_w as a function of the liquid volume, V^*. $L_0^* = 16.6$ cm (static loading: numerical results).

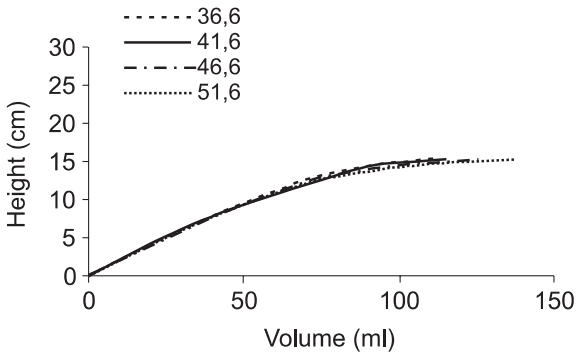

Fig. 12. Variation of the liquid height, l_w, as a function of the liquid volume, V^*. $L_0^* = 11.6$ cm. Membrane rotating at a constant angular velocity $\omega = 40$ rad/s (numerical resuslts).

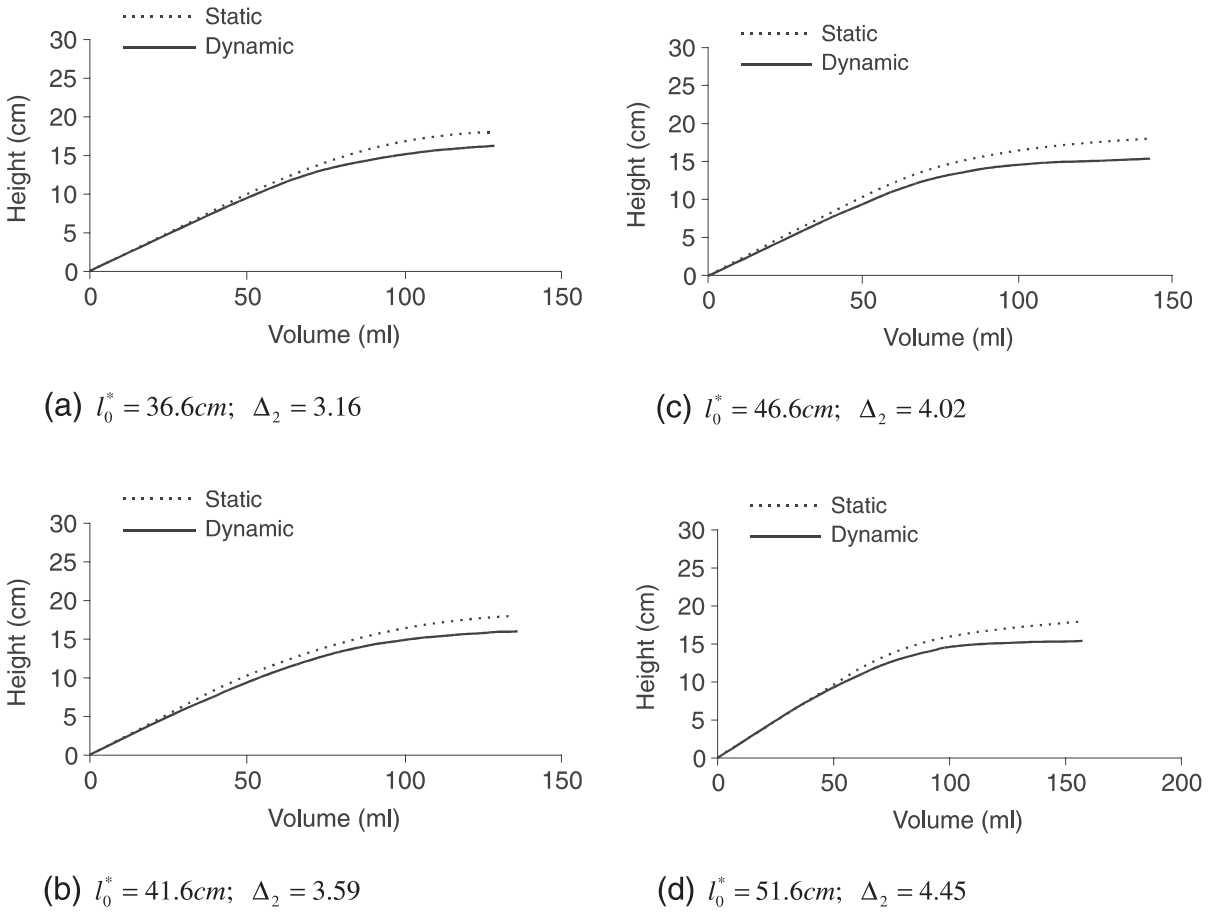

Fig. 13. Numerical analysis: comparision between static and dynamic results, $L_0^* = 11.6$ cm.

values of l_0^*. It is observed that, as the volume increases gradually, the height of water increases until a limit value is reached, after which the volume can increase continuously without any perceptible increase in the related height of water. In all the results presented here, the influence of the initial stress state, expressed by the overall extension ratio $\Delta_2 = l_0^*/L_0^*$, was found to be very small, with all the curves almost the same.

The numerical results for the membrane rotating at a constant angular velocity are shown in Fig. 12 for $L_0^* = 11.6$ cm. Here it is possible to see that the height of water increases with the volume up to a maximum value – but it was not possible to obtain numerically the descending branch of the curve since the numerical algorithm, as implemented here, is not capable of passing a limit point. The comparison between the numerically obtained values for the static and dynamic cases is shown in Fig. 13 for $L_0^* = 11.6$ cm where again it is observed that for the same volume of water, the height of water is lower for the rotating tube than for the static case. This agrees with the experimental results shown previously.

4.1. Comparison between experimental and numerical results

The comparison between the experimental and numerical results for the static case is shown in Figs. 14 and 15. There is an excellent agreement between theory and experiment for low values of the extension ratio

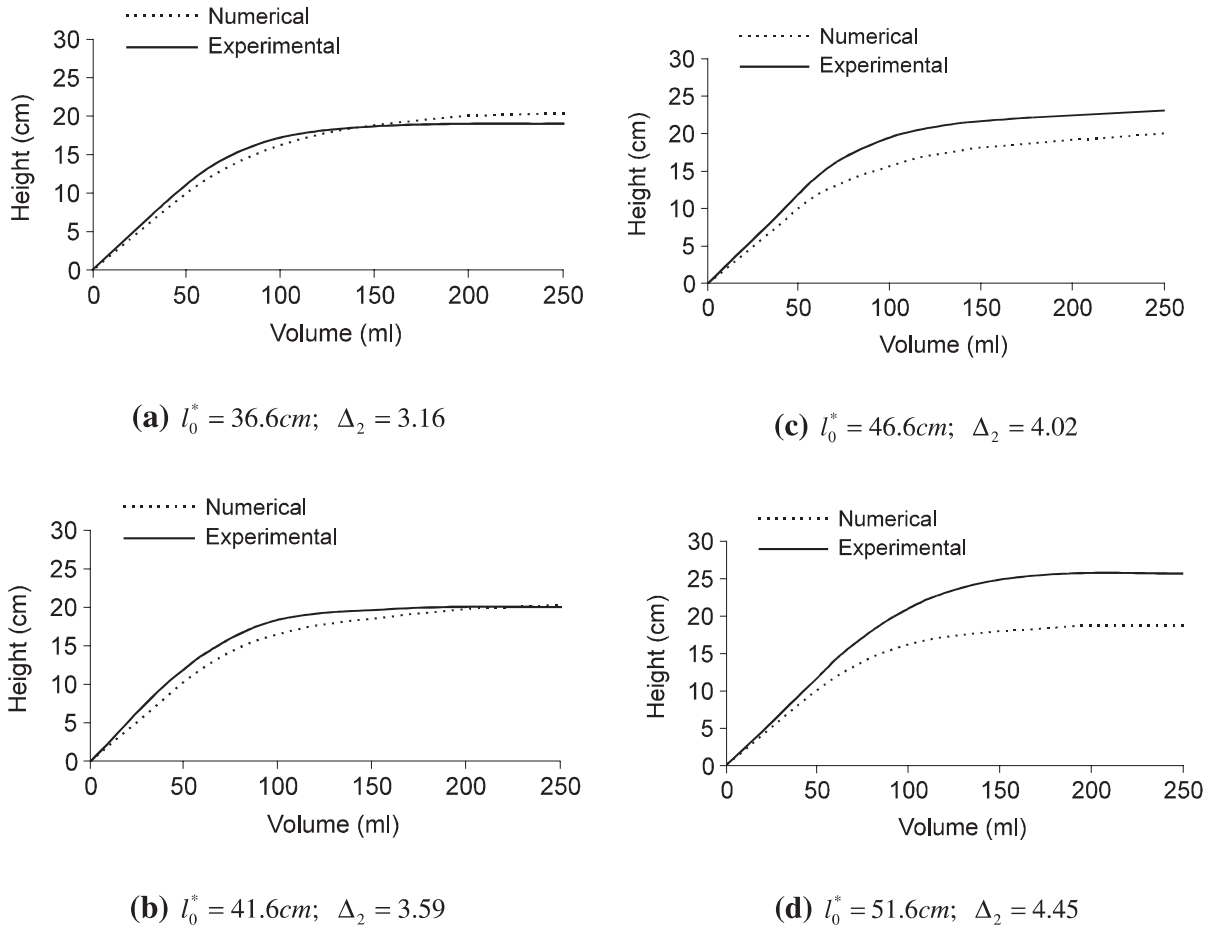

Fig. 14. Comparision between experimental and numerical results: static case. $L_0^* = 11.6$ cm.

$\Delta_2 = l_0^*/L_0^*$. On the other hand, for values of Δ_2 higher than four there is, as shown in Fig. 14c and d, a noticeable difference between the numerical and experimental curves. For the tube with initial length of 16.6 cm, Fig. 15, since the values of Δ_2 are relatively small, the experimental and numerical results are in very good agreement. We believe that for large values of Δ_2 it is possible to improve the correlation between the numerical and experimental results by changing the constitutive relation of the material. In a previous study using rubber membranes, Pamplona and Bevilacqua (1992) observed that for large extension ratios, the Mooney–Rivlin constitutive model gives better results when compared with the experimental ones than the neo-Hookean model used in this paper. The comparison between the experimental and numerical results for the rotating membrane are not so good, but even in this case the numerical results present the same qualitative behaviour, as illustrated in Fig. 16.

5. Discussion and conclusion

In this work, the finite deformations of an isotropic circular cylindrical membrane subjected to a finite extension and gradually filled with liquid were investigated both theoretically and experimentally.

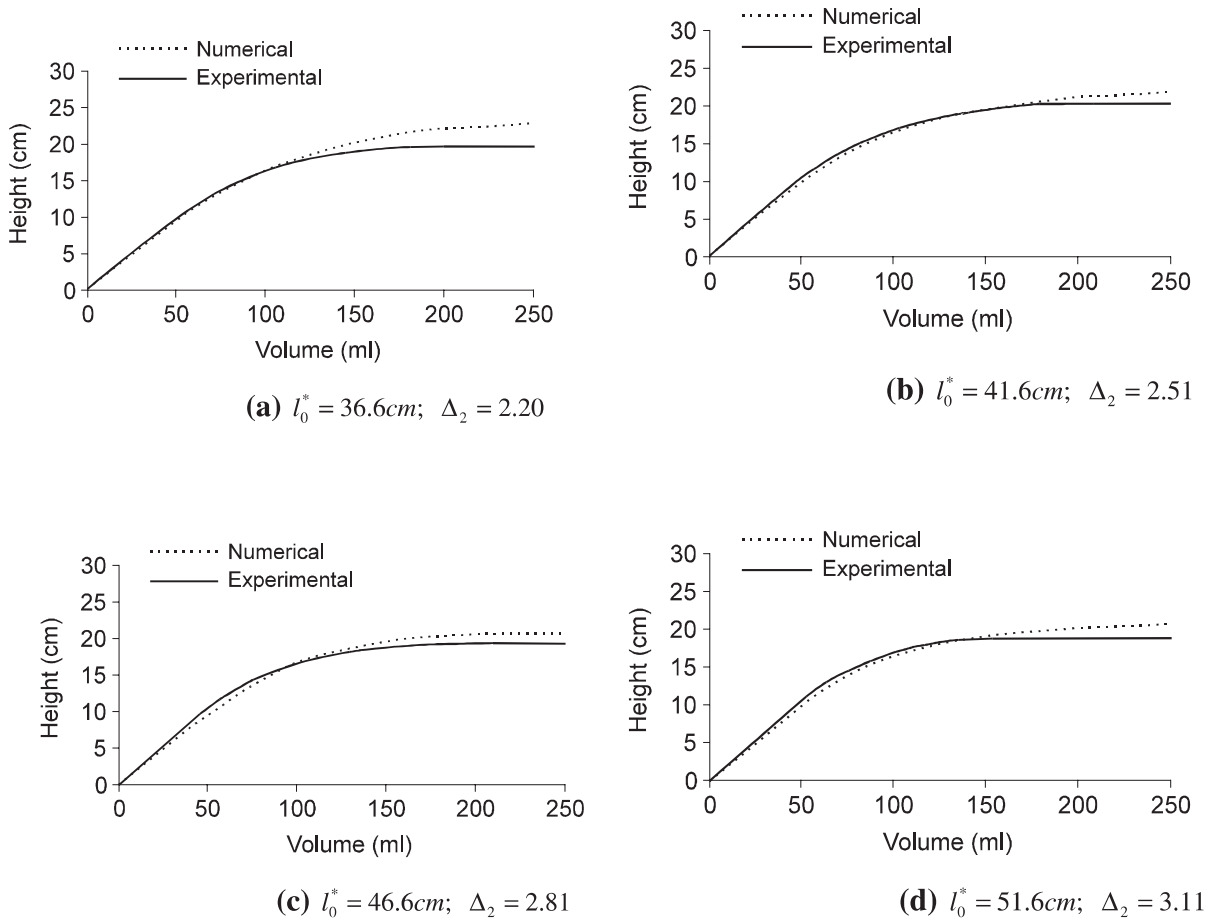

Fig. 15. Comparision between experimental and numerical reuslts: static case. $L_0^* = 16.6$ cm.

Theoretical and, particularly, experimental investigations of membranes under variable pressure are scarce in the literature. Nonetheless, this is a problem of importance in many engineering fields including some relevant biomedical problems. The agreement of the experimental and numerical results, especially for relatively low values of the extension ratio Δ_2, is rather encouraging and indicates that the present formulation can satisfactorily model the deformation field under consideration. Also the experimental results presented here, covering a large collection of cases, can be used as a benchmark for future theoretical and numerical works in this area.

Two important phenomena were observed during the experiments: (a) the existence, for certain extended membranes, of a maximum hydrostatic pressure (or liquid height) and (b) the loss of stability of the axisymmetric deformed configuration at a critical liquid volume, both in the static and dynamic cases. As observed experimentally, as water is added, the membrane deforms symmetrically and the liquid height increases continuously until a maximum height and, consequently, hydrostatic pressure is reached. At this point, the addition of more liquid causes increased symmetric deformation near the base of the tube while the liquid height remains practically constant. This maximum height is a function of the ratio between the initial and final length of the membrane, Δ_2. For relatively low values of Δ_2, this critical height is practically constant but increases for large values of Δ_2.

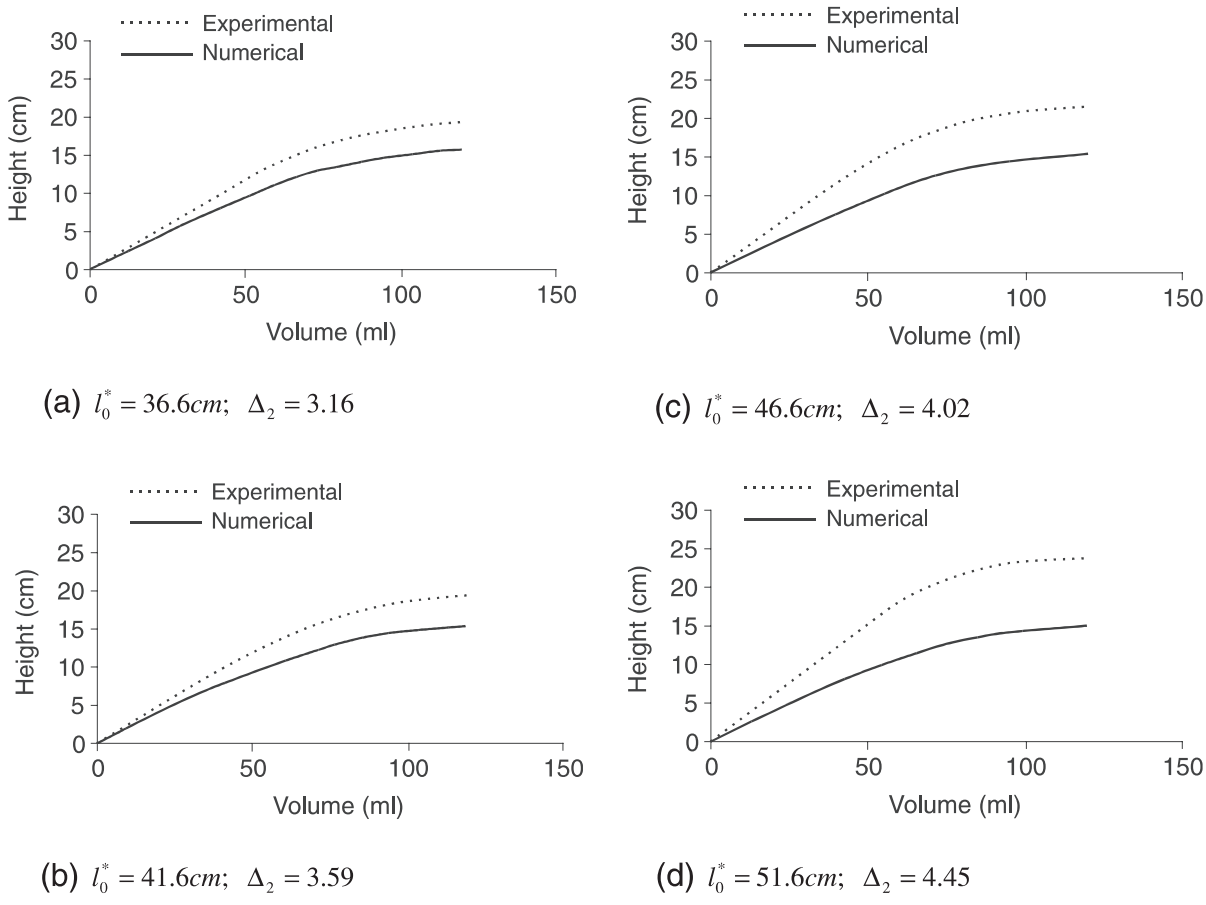

Fig. 16. Comparison between experimental and numerical results: rotating membrane. $L_0^* = 11.6$ cm; $\omega = 40$ rad/s.

Finally, the volume of the internal fluid reaches a critical value causing a bifurcation into an asymmetric mode. After the bifurcation a major part of the liquid passes on one side of the symmetry axis with a sudden decrease in the hydrostatic pressure.

Since the observed instability mode is not rotationally symmetric, the present numerical formulation allows no prediction of when a critical configuration will occur. This study is a natural extension of the present work and will be performed in the near future.

References

Alexander, H., 1971. Tensile instability of initially spherical balloons. Int. J. Engng. Sci. 9, 151–162.

Boyer, D.L., Gutkowski, W., 1970. Liquid filled membranes. Int. J. Non-Linear Mechanics 5, 299–310.

Chen, Y., 1995. Stability and bifurcation of inflated cylindrical elastic membranes. In: Godoy, L.A., Idelshon, S.R., Laura, P.A.A., Mook, D.T. (Eds.), Applied Mechanics in the Americas, vol. 1, pp. 404–409.

Corneliussen, A.H., Shield, R.T., 1961. Finite deformation of elastic membranes with application to the stability of an inflated and extended tube. Archs. Ration. Mech. Analysis 1, 273–304.

Dos Anjos, A.M.G., Gonçalves, P.B., 1996. Large deflection, geometrically non-linear analysis of arches and beams. In: Rondal, J., Dubina, D., Gioncu, V. (Eds.), Coupled Instabilities in Metal Structures, Imperial College Press, pp. 69–76.

Green, A.E., Adkins, J.E., 1960. Large Elastic Deformations and Non-Linear Continuum Mechanics. Oxford University Press, Oxford, MA.

Evans, E.A., Skalak, R., 1981. Mechanics and Thermodynamics of Biomembranes. CRC Press, Boca Raton, Florida.

Haseganu, E.M., Steigmann, D.J., 1994. Theoretical flexure of a pressurized cylindrical membrane. Int. J. Solids Struct. 31, 27–50.

Haughton, D.M., Ogden, R.W., 1978. On the incremental equations in non-linear elasticity – II: Bifurcation of pressurized spherical shell. J. Mech. Phys. Solids 26, 111–138.

Haughton, D.M., 1996. Axially elastic membranes subjected to fluid loads. IMA J. Appl. Math. 56, 303–320.

Isaacson, M., 1987. Transportation of fresh water by sea to San Diego from Northern California. Technical Report, Altaplan, Calgary, Alberta.

Keller, H.B., 1968. Numerical Methods for Two-Point Boundary-Value Problems. Blaisdell, Waltham, MA.

Krayterman, B.L., 1990. Nonlinear analyses of axisymmetric membranes with shooting method. J. Struct. Engng., ASCE 116, 1857–1876.

Li, X., Steigmann, D.J., 1993. Finite plane twist of an annular membrane. Q. J. Mech. Appl. Math. 46, 601–626.

Ohyama, T., Tanaka, M., Kiyokawa, T., Uda, T., Murai, T., 1989. Transmission and reflection characteristics of waves over a submerged flexible mound. Coastal Engng. Japan 32, 53–68.

Pamplona, D., Bevilacqua, L., 1992. Large deformations under axial force and moment load of initially flat membranes. Int. J. Non-Linear Mechanics 27, 639–650.

Pamplona, D., Calladine, C.R., 1993. The mechanics of axially symmetric liposomes. J. Biomech. Engng. 115, 149–159.

Press, W.H., Flannery, B.P., Teukolsky, S.A., Vetterling, W.T., 1986. Numerical Recipes. Cambridge University Press, UK.

Ratner, A.M., 1983. Tensile stability of cylindrical membranes. Int. J. Non-Linear Mechanics 18, 133–147.

Secomb, T.W., Gross, J.F., 1983. Flow of red blood cells in narrow capillaries: Role of membrane tension. Int. J. Microcirc. Clin. Exp. 2, 229–240.

Treolar, L.R.G., 1975. The Physics of Rubber Elasticity. Oxford University Press, UK.

Williams, A.N., 1996. Floating membrane breakwater. J. Offshore Mechanics and Artic Engng., ASME 118, 46–51.

Yu, L.K., Valanis, K.C., 1970. The inflation of axially symmetric membranes by linearly varying hydrostatic pressure. Trans. Soc. Rheol. 14, 159–183.

Zhao, R., 1995. A complete linear theory for a two-dimensional floating and liquid-filled membrane structure in waves. J. Fluids and Structures 9, 937–947.